Chinese Journal of Chemical Engineering 23 (2015) 15–21

Contents lists available at ScienceDirect

Chinese Journal of Chemical Engineering

journal homepage: www.elsevier.com/locate/CJCHE

Fluid Dynamics and Transport Phenomena

Numerical simulation of steady flow past a liquid sphere immersed in simple shear flow at low and moderate *Re* ☆

Run Li [1], Jingsheng Zhang [1,2], Yumei Yong [1], Yang Wang [1,*], Chao Yang [1,*]

[1] Key Laboratory of Green Process and Engineering, Institute of Process Engineering, Chinese Academy of Sciences, Beijing 100190, China
[2] Beijing Research Institute of Chemical Industry, SINOPEC, Beijing 100013, China

ARTICLE INFO

Article history:
Received 28 March 2013
Received in revised form 15 April 2013
Accepted 28 April 2014
Available online 30 October 2014

Keywords:
Shear flow
Liquid sphere
Numerical simulation
Streamline
Jeffery orbit

ABSTRACT

This work presents a numerical investigation on steady internal, external and surface flows of a liquid sphere immersed in a simple shear flow at low and intermediate Reynolds numbers. The control volume formulation is adopted to solve the governing equations of two-phase flow in a 3-D spherical coordinate system. Numerical results show that the streamlines for $Re = 0$ are closed Jeffery orbits on the surface of the liquid sphere, and also closed curves outside and inside the liquid sphere. However, the streamlines have intricate and non-closed structures for $Re \neq 0$. The flow structure is dependent on the values of Reynolds number and interior-to-exterior viscosity ratio.

1. Introduction

Shear flow generally exists in multiphase dispersions in process industry. In some practical cases, a liquid sphere (droplet) subjects to the force of gravity and shear simultaneously. For example, the droplets in a stirred tank would bear shear force from the continuous phase at low and moderate *Re* (*e.g.*, in high viscous systems and fine emulsions). Convection and shear have appreciable effects on the transport processes at moderate Reynolds numbers. A thorough understanding of the flow structure around a single droplet in simple shear flow would help in gaining insight into the transport process of a droplet in pure shear and complex flows. The research on pure shear flow at low and moderate *Re* would also help us to understand the complex interaction of shear and advection co-existing in general liquid–liquid systems. The internal and external flow fields of dispersed phase particles (including bubble and drop) would display special flow structures in shear flows. Thus it is necessary to study the fluid mechanics of a single particle in shear flows for extensive understanding of rheological properties of multiphase dispersions. On the other hand, mass and heat transfer correlates closely with the inside and outside flow fields. This motivates the present study on the flow structures around single particles.

Peery [1] used a singular perturbation technique to study the effect of weak fluid inertia on the fluid velocity field around a rigid or deformable sphere in simple shear flow. Roberson and Acrivos [2] investigated theoretically and experimentally the fluid velocity field around a freely suspended cylinder in simple shear flow at low Reynolds numbers and found that the region of closed streamlines had a finite extent along the direction of flow. Poe and Acrivos [3] studied a solid sphere rotating freely in simple shear flow experimentally for moderate values of Reynolds number up to 10 and obtained the rotation rates of such a sphere. Subramanian and Koch [4] deduced that the fluid inertia made streamlines near a solid sphere open at non-zero *Re*, instead of remaining closed as in the case of $Re = 0$. For non-zero but very small *Re*, centrifugal forces caused the streamlines in the flow-gradient plane spiral away from the particle surface. Mikulencak and Morris [5] quantified the particle rotation rate for a solid sphere in simple shear flow and its contribution to the fluid stress by using a finite element method. Yang *et al.* [6] studied similar problem numerically by a finite difference method and their numerical results of particle rotation rate were consistent with those of Mikulencak and Morris [5]. These theoretical analyses [5,6] were limited to $Re \ll 1$ and solid spheres. Liquid spheres immersed in simple shear flow at intermediate *Re* are seldom targeted. The numerical results of velocity and stress [6] have been used to analyze the stresslet for liquid spheres [7]. Mao *et al.* [8] investigated numerically the fully developed steady flow of non-Newtonian yield viscoplastic fluid through concentric and eccentric annuli. The fluid rheology is described with the Herschel–Bulkley model. The numerical simulation based on a continuous viscoplastic approach to the Herschel–Bulkley model is found in poor accordance with the experimental data on

☆ Supported by the National Basic Research Program of China (2013CB632601), the National Science Fund for Distinguished Young Scholars (21025627), the National Natural Science Foundation of China (21276256, 21106150) and the National High Technology Research and Development Program of China (2012AA03A606).
* Corresponding authors.
E-mail addresses: wangyang@ipe.ac.cn (Y. Wang), chaoyang@ipe.ac.cn (C. Yang).

http://dx.doi.org/10.1016/j.cjche.2014.10.005
1004-9541/

volumetric flow rate of a bentonite suspension. Fan and Yin [9] investigate the interaction of two bubbles rising side by side in shear-thinning fluid using volume of fluid (VOF) method coupled with continuous surface force (CSF) method. By considering rheological characteristics of fluid, this approach was able to accurately capture the deformation of bubble interface, and validated by comparing with the experimental results.

In this work, we determine numerically the flow field around a neutrally buoyant liquid sphere in simple shear flow at finite Reynolds numbers with a control volume formulation. We present in detail the flow fields inside and outside a liquid sphere in simple shear and the flow structure on drop surface. It is believed that the flow features revealed by numerical simulation will be useful for further analysis of heat and mass transfer as well as liquid–liquid chemical reactions.

2. Model Equations and Method

A rigid liquid sphere is placed at the origin of coordinate system in a Newtonian fluid, which is subject to simple constant shear far from the droplet. The continuous and dispersed phases have equal densities. The flow field without the central sphere is given in the Cartesian coordinates as $\boldsymbol{u}' = (\dot{\gamma} y, 0, 0)$, where $\dot{\gamma}$ is the velocity gradient of simple shear flow. Flow circulations may exist inside a liquid sphere due to the shear stress from the continuous phase. The physical properties of two phases may be different. In the laminar flow regime, the velocity ($\boldsymbol{u}$) and pressure (p) in each phase are governed by the continuity and Navier–Stokes equations, in dimensionless form, as follows

$$\nabla \cdot \boldsymbol{u}_1 = 0, \qquad \boldsymbol{u}_1 \cdot \nabla \boldsymbol{u}_1 = -\nabla p_1 + \frac{1}{Re_1}\nabla^2 \boldsymbol{u}_1 \tag{1}$$

$$\nabla \cdot \boldsymbol{u}_2 = 0, \qquad \boldsymbol{u}_2 \cdot \nabla \boldsymbol{u}_2 = -\nabla p_2 + \frac{1}{Re_2}\nabla^2 \boldsymbol{u}_2 \tag{2}$$

where the subscript $i = 1$ is for the droplet and $i = 2$ for the continuous phase. Coordinates are non-dimensionalized by liquid sphere radius a, velocity by $a\dot{\gamma}$, and stresses by $\mu\dot{\gamma}$, where μ is the viscosity of continuous phase. The Reynolds number is defined by $Re_i = \dot{\gamma} a^2 \rho_i / \mu_i$, the viscosity ratio by $\lambda = \mu_1/\mu_2$, and ρ is the density of both liquids.

The spherical coordinate system in this work is illustrated in Fig. 1, with azimuthal angle coordinate φ, polar angle coordinate θ and radial coordinate r. The boundary conditions related to this problem are as follows.

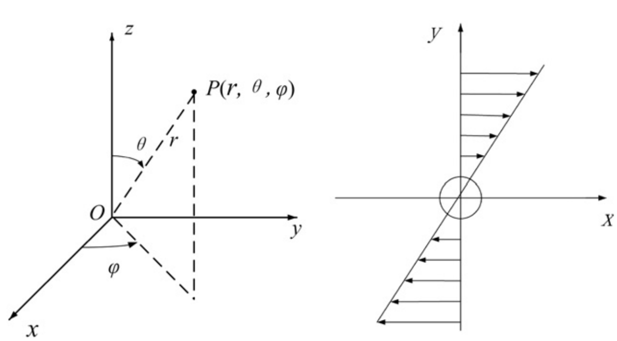

Fig. 1. Projected image of the target system and flow direction of continuous phase.

(1) At the droplet interface, the normal velocity is 0:

$$r = 1, \quad (u_{1r})_s = (u_{2r})_s = 0. \tag{3}$$

The tangential velocity is continuous:

$$\begin{aligned} r = 1, \quad (u_{1\theta})_s &= (u_{2\theta})_s \\ r = 1, \quad \left(u_{1\varphi}\right)_s &= \left(u_{2\varphi}\right)_s \end{aligned}. \tag{4}$$

The tangential stresses are in balance:

$$\begin{aligned} r = 1, \quad (\tau_{1r\theta})_s &= (\tau_{2r\theta})_s \\ r = 1, \quad \left(\tau_{1r\varphi}\right)_s &= \left(\tau_{2r\varphi}\right)_s \end{aligned}. \tag{5}$$

where the shear stress is computed by

$$\begin{aligned} \tau_{1r\theta} &= \left[\frac{1}{r}\frac{\partial u_{1r}}{\partial \theta} + r\frac{\partial}{\partial r}\left(\frac{u_{1\theta}}{r}\right)\right], \tau_{2r\theta} = \lambda\left[\frac{1}{r}\frac{\partial u_{2r}}{\partial \theta} + r\frac{\partial}{\partial r}\left(\frac{u_{2\theta}}{r}\right)\right] \\ \tau_{1r\varphi} &= \left[\frac{1}{r\sin\theta}\frac{\partial u_{1r}}{\partial \varphi} + r\frac{\partial}{\partial r}\left(\frac{u_{1\varphi}}{r}\right)\right], \\ \tau_{2r\varphi} &= \lambda\left[\frac{1}{r\sin\theta}\frac{\partial u_{2r}}{\partial \varphi} + r\frac{\partial}{\partial r}\left(\frac{u_{2\varphi}}{r}\right)\right]. \end{aligned} \tag{6}$$

(2) At the outer boundary of the field,

$$r \rightarrow \infty, \quad \boldsymbol{u}_1 = \boldsymbol{u}^{\infty} = (y/a, \ 0, \ 0). \tag{7}$$

(3) At $\theta = 0°$ and 180°, the velocity vector is continuous [10]:

$$\boldsymbol{u}_1(i_0, j, k_0) = \frac{1}{N_\varphi}\sum_{k=1}^{N_\varphi} \boldsymbol{u}_1(i_0 + 1, j, k). \tag{8}$$

(4) At $\varphi = 0°$ and 360°, the velocity is continuous:

$$\boldsymbol{u}_{1,\ \varphi=0} = \boldsymbol{u}_{1,\ \varphi=2\pi}. \tag{9}$$

(5) At the center of the droplet ($r = 0$), the flow is also continuous:

$$\boldsymbol{u}_{1,r=0} = \frac{1}{N_\theta N_\varphi}\sum_{j=1}^{N_\theta}\sum_{k=1}^{N_\varphi} \boldsymbol{u}_1(\Delta r, j, k). \tag{10}$$

In this study, Eqs. (1) and (2) are solved by a finite volume method in a three-dimensional spherical coordinate system. The computational domain is $0 \le r \le R$, $0 \le \theta \le \pi$ and $0 \le \varphi \le 2\pi$, where R is the size of computing domain in the radial direction. At small Re the outer boundary must be larger than the length scale $aRe^{-1/2}$ on which the inertial and viscous terms are comparable. For larger particle Reynolds numbers, the computing domain should cover the area where the vorticity exists. Governing Eqs. (1) and (2) are discretized on a staggered grid, with the nodes for u_r allocated on the drop surface and the origin. The grid is uniform in azimuthal (φ) and polar (θ) directions, but non-uniform in radial (r) direction. For the internal domain, 10–20 nodes are allocated densely and uniformly in the r direction near the surface inside the sphere, whereas away from the surface the nodes are distributed uniformly but with a larger spacing. For the external domain, 20–30 nodes in the r direction are set closely and uniformly near the surface since the velocity boundary is very thin, but after that an exponential expansion of cell size is applied: $r(n) = r(n-1)e^{\alpha}$, where α is a small constant used to adjust the node spacing.

The control volume formulation with the SIMPLE algorithm [9] is adopted to solve the governing equations. Although $\theta = 0°$ and 180° and $\varphi = 0°$ (360°) are boundaries of the computational domain, the fluid flow is continuous there. The values of u and p are specified iteratively as suggested as Zhang *et al.* [6]. Grid sensitivity analysis has proved that $R = 60a$ and a grid with [60(internal) + 150(external)] $(r) \times 30(\theta) \times 60(\varphi)$ (the minimum $\Delta r = 0.0025$) suffices for computational accuracy.